PROCEEDINGS OF SCIENCE

Test of lepton flavour universality with semi-tauonic decays of b-hadrons at LHCb

Anna Lupato[*†]
Università degli Studi di Padova and INFN - Padova, Italy
E-mail: anna.lupato@pd.infn.it

Lepton Flavour Universality (LFU) is enforced in the Standard Model by construction. Any violation of LFU would be a clear sign of new physics. Existing hints of non universality are already present. The semitauonic decays in particular, are sensitive to contributions from non-Standard-Model particles that preferentially couple to the third generation of fermions, such as Higgs-like charged scalars. The LHCb experiment has measured the branching fraction ratio $R(D^*) \equiv \mathscr{B}(\bar{B}^0 \to D^{*+}\tau^-\bar{\nu}_\tau)/\mathscr{B}(\bar{B}^0 \to D^{*+}\mu^-\bar{\nu}_\mu)$ using a sample of proton-proton collision data corresponding to an integrated luminosity of $3fb^{-1}$ recorded until 2012. Only muonic tau decays, $\tau^- \to \mu^-\bar{\nu}_\mu\nu_\tau$, are considered. The ratio is measured to be $R(D^*) = 0.336 \pm 0.027(stat) \pm 0.030(syst)$, which is 2.1 standard deviations larger than the value expected from lepton universality in the Standard Model.

XIII International Conference on Heavy Quarks and Leptons
22- 27 May, 2016
Blacksburg, Virginia, USA

[*]Speaker.
[†]On behalf of the LHCb Collaboration

PoS(HQL 2016)066

1. Introduction

Lepton flavour Universality (LFU) implies equality of coupling between the gauge bosons and the three families of leptons. It implies that the branching fractions of e, μ and τ differ only by phase space and helicity-suppressed contributions. Lepton Flavour Unversality is enforced in the Standard Model (SM) by construction and therefore, any violation would be a clear sign of New Physics. Over the years, the LFU has been tested but has proven to be an accurate description in several systems. Recent hints of lepton non-universal effects in $B^+ \to K^+e^+e^-$ and $B^+ \to K^+\mu^+\mu^-$ decays have been seen, but these are not definitive observations yet [1]. A large class of models extending the SM contain additional interaction involving enhanced couplings to the third generation which would violate the universality. An extended Higgs Sector could have a large effect on semitauonic decay rates through the coupling of new charged Higgs scalars [2, 3]. Therefore, semileptonic decays of b hadrons to the third generation provide a sensitive probe for such effects. In particular, a theoretically clean observable is the ratio:

$$R(D^*) \equiv \frac{\mathscr{B}(\bar{B}^0 \to D^{*+}\tau^-\bar{\nu}_\tau)}{\mathscr{B}(\bar{B}^0 \to D^{*+}\mu^-\bar{\nu}_\mu)}$$

Indeed, this ratio is independent of V_{cb} and depends on hadronic physics only in the ratio of form factors, whose uncertainties due to ratio are canceled. It is currently predicted to be $R(D^*) = 0.252 \pm 0.003$ [3]. Experimentally, this measurement is clean considering muonic tau decays, $\tau^- \to \mu^-\bar{\nu}_\mu\nu_\tau$, since $\mathscr{B}(\tau^- \to \mu^-\bar{\nu}_\mu\nu_\tau) = 17.41\%$ [4].

The signal decays, $\bar{B}^0 \to D^{*+}\tau^-\bar{\nu}_\tau$ and the normalization channel $\bar{B}^0 \to D^{*+}\mu^-\bar{\nu}_\mu$ produce identical visible particles in the final states, therefore the relative efficiencies of the two channels depend only on the differing kinematics and the reconstruction, particle identification and tracking efficiencies cancel to first order.

Until 2015, only B-factories, BaBar and Belle measured $R(D^*)$ and the $R(D)$, obtaining a combined average measure which is 3.4 standard deviation greater than Standard Model prediction (2.7σ and 2σ respectively) [5, 6].

2. LHCb

The LHCb detector [7, 8] is a single-arm forward spectrometer covering the pseudorapidity range $2 < \eta < 5$, designed for the study of particles containing b or c quarks. The detector includes a high-precision tracking system consisting of a silicon-strip vertex detector surrounding the pp interaction region [8], a large-area silicon-strip detector located upstream of a dipole magnet with a bending power of about 4 Tm, and three stations of silicon-strip detectors and straw drift tubes placed downstream of the magnet [9]. The combined tracking system provides a momentum measurement with a relative uncertainty that varies from 0.4% at low momentum to 0.6% at 100 Gev/c, and an impact parameter measurement with a resolution of 20 μm for charged particles with large transverse momentum, p_T. Different types of charged hadrons are distinguished using information from two ring-imaging Cherenkov detectors [11]. Photon, electron and hadron candidates are identified by a calorimeter system consisting of scintillating-pad and pre-shower detectors, an electromagnetic calorimeter and a hadronic calorimeter. Muons are identified by a system composed

of alternating layers of iron and multi-wire proportional chambers [12]. The trigger [13] consists of a hardware stage, based on information from the calorimeter and muon systems, followed by a software stage, which applies a full event reconstruction.

3. The $R(D^*)$ measurement at LHCb

A precise measurement of a B decay involving τ leptons is a challenge at an hadron collider and was never performed before at LHCb. This is due to the presence of large partially reconstructed B backgrounds, and in particular, the presence of additional, non-reconstructed decay products cannot be excluded. Moreover, the b hadron kinematics can not be constrained due to unknown parton-parton collision energy and the neutrinos in the final states.

The $R(D^*)$ LHCb analysis uses a sample of proton-proton collision data corresponding to $3\,\text{fb}^{-1}$ of integrated luminosity recorded by LHCb during 2011 and 2012 at $\sqrt{s} = 7$ TeV and $\sqrt{s} = 8$ TeV. Only muonic decays of τ are considered and the D^{*+} mesons are reconstructed in the $D^{*+} \to (D^0 \to K^-\pi^+)\pi^+$ decay mode. The signal and normalization channel decays exploit the excellent capabilities of the LHCb detector concerning momentum, impact parameter resolution and particle identification.

The trigger requirements are chosen to avoid the requirement of any selection on muon p_T or on $D^{*+}\mu^-$ to not bias the $\bar{B}^0 \to D^{*+}\tau^-\bar{\nu}$ kinematic distributions. The software trigger selection is focused on reconstruction of $D^0 \to K^-\pi^+$ with high p_T and displaced vertex with respect to primary vertex.

The overall efficiencies ratio, after the full selection, is found to be $\varepsilon_\tau/\varepsilon_\mu = (77.6 \pm 1.4)\%$, since the tau decays, where the tauonic decay is less efficient due to low p_T of secondary muon and worse vertex quality of signal decay.

In a semileptonic decay at a hadron collider, due to the presence of one or more neutrinos, is not possible to reconstruct the B momentum in the laboratory rest frame using final particles and therefore constrain the kinematics of decay. Hence, it is necessary to use an approximation. In this analysis, the hadron momentum in the B rest frame is calculated using the B momentum direction, determined from the unit vector to B decay vertex from the associated primary vertex and assuming that the proper velocity $\beta\gamma$ of visible part of semileptonic decay along z-axis is equal to B proper velocity along the same axis [14]

$$(p_B)_z = (p_{D^*\mu})_z \frac{m_B}{m_{D^*\mu}}$$

$$|p_B| = (p_{D^*\mu})_z \frac{m_B}{m_{D^*\mu}} \sqrt{(1+\tan^2\alpha)}$$

where is α is the angle between unit vector and z axis (beam pipe) [14] .

The main background sources for the signal and normalization channel consist of partially reconstructed B decays. The most dangerous are $\bar{B}^0 \to D^{**+}\mu^-\bar{\nu}_\mu$, $\bar{B}^0 \to D^{*+}n\pi\mu^-\bar{\nu}_\mu$ and $\bar{B}^0 \to D^{*+}H_cX$ with any possible $H_c \to Y\mu\nu$. To suppress the contributions of partially reconstructed B decays, an algorithm is developed to determine whether a given track is likely to have originated

from the signal B candidate or from the rest of events. The $D^{*+}\mu$ candidates are required to be isolated from additional tracks in the event. By requiring zero additional tracks at B vertex, the selected data sample is enriched in $\bar{B}^0 \to D^{*+}\tau^-\bar{\nu}_\tau$ and $\bar{B}^0 \to D^{*+}\mu^-\bar{\nu}_\mu$. By requiring one or two additional tracks originated from B vertex, data sample is enriched in $\bar{B}^0 \to D^{*+}X\pi\mu^-\bar{\nu}_\mu$. Finally, if at least one of selected track satisfies kaon identifications requirements a sample enriched in $\bar{B}^0 \to D^{*+}K^{\pm}X\mu^-\bar{\nu}_\mu$ is obtained. These samples are used to study the shapes of background components.

The separation of the signal from the normalization channel is achieved by exploiting the distinct kinematic distributions that characterize the two decay modes, resulting from the differences in masses between the muon and the tau particles and from presence of three neutrinos in the tau decay mode. In the B rest frame, the following quantities allow us to distinguish signal from muonic decay: the missing mass squared $m^2_{miss} = (p^\mu_B - p^\mu_D - p^\mu_\mu)^2$, E^*, the energy of muon in the center of mass of B and the transferred momentum $q^2 = (p^\mu_B - p^\mu_D)^2$, where p^μ_i is the four-momentum of particle i [14] .

The distributions of discriminating variables extracted by a simulated sample and the corresponding quantities are reconstructed using B momentum approximation, previous described, have been compared. The resolution is about $15-20\%$, and the distributions preserve their discriminating power, as seen in Fig. 1.

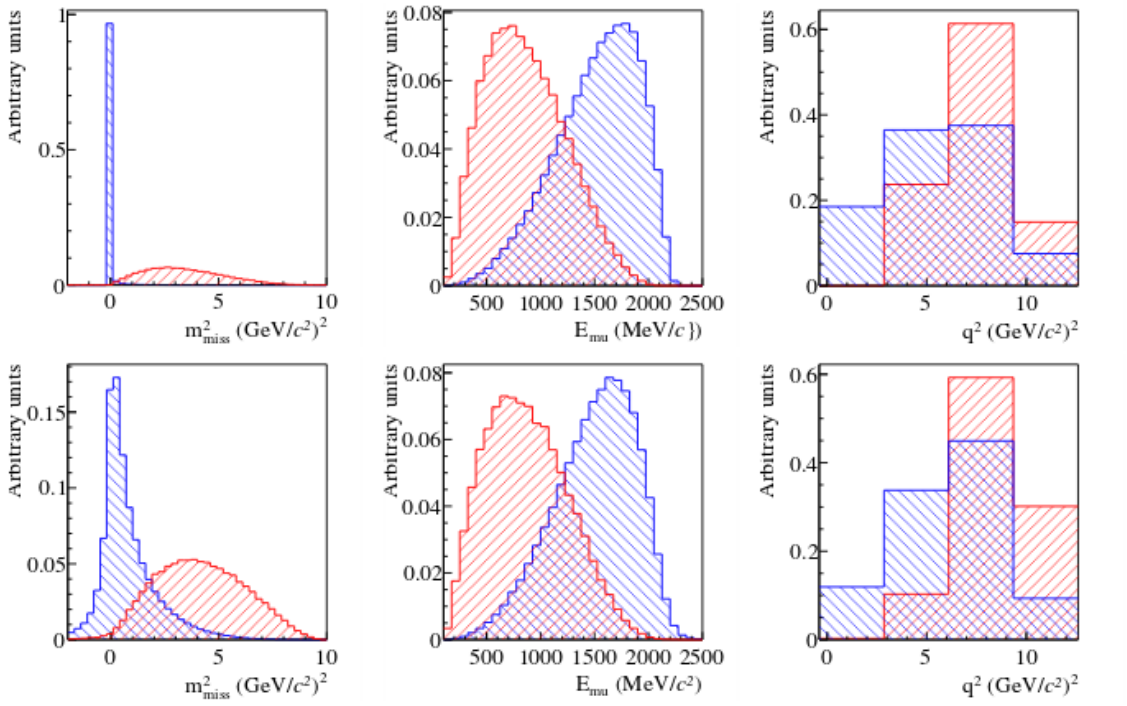

Figure 1: From left to right: Distributions of m^2_{miss}, missing mass squared; E^*, the energy of muon in the center of mass of B and the momentum transferred q^2 for the simulated $\bar{B}^0 \to D^{*+}\tau^-\bar{\nu}_\tau$ (red) and $\bar{B}^0 \to D^{*+}\mu^-\bar{\nu}_\mu$ (blue) using MC truth (top) and reconstructed (bottom) quantities.

The binned m^2_{miss}, $E^*$and q^2 distributions in data are fit using a maximum likelihood method with three dimensional templates representing the signal $\bar{B}^0 \to D^{*+}\tau^-\bar{\nu}_\tau$, the normalization channel

$\bar{B}^0 \to D^{*+}\mu^-\bar{\nu}_\mu$ and the background sources. The binning of the templates is the following: 40 bins for m^2_{miss} distribution in the kinematic region $2 < m^2_{miss} < 10$ GeV$^2/c^4$, 30 bins of E^* distribution in the range $100 < E^* < 2500$ MeV and finally the q^2 distribution is binned in 4 bins in the range $-0.4 < q^2 < 12.6$ GeV$^2/c^4$.

All uncertainties on the template shapes are incorporated in the fit. The uncertainties due to finite number of simulated events are incorporated in the likelihood using the Beeston Barlow "lite" procedure [16]. The shapes uncertainties, instead, are included via interpolation between nominal and alternative histograms.

The hadronic transition-matrix elements for $\bar{B}^0 \to D^{*+}\tau^-\bar{\nu}_\tau$ and $\bar{B}^0 \to D^{*+}\mu^-\bar{\nu}_\mu$ are described using form factors derived from heavy quark effective theory [15].

The choice of the model for the templates of each background is validated on fits to separated control samples, the ones obtained by applying alternative requirements to multivariate analysis.

For the background semileptonic decays $\bar{B}^0 \to D_1(2420), D_2^*(2460), D_1'(2430)\mu^-\bar{\nu}_\mu$ separate templates are defined with form factors taken from Ref. [17]. The slope of Isgur-Wise function is included as a free parameter in the fit, with a constraint derived from fitting the $D^{*+}\pi\mu^-\bar{\nu}_\mu$ control sample. Semileptonic decays to heavier charmed hadrons decaying as $D^{**} \to D^*\pi\pi$ is modeled using the ISGW2 parametrization [18]. Since resonances which contribute to final states and their form factors are not known, a fit on $D^{*+}\pi\pi\mu^-\bar{\nu}_\mu$ control sample allows to obtain an empirical correction to the q^2 distribution. Similar parametrizations are used for semitauonic D^{**} decay modes. The contribution of $\bar{B}^0 \to D^{**+}\mu^-\bar{\nu}$ background amounts to about 12% of the normalization mode in the fit to signal sample [14].

Other processes which occur at about $6-8\%$ of the normalization mode are $\bar{B}^0 \to D^{*+}H_cX$ with any possible $H_c \to Y\mu\nu$. Aimed to model these processes, the templates are generated using a cocktail of simulated B^0 and B^+ decay in appropriate final states. Corrections to templates are obtained by fitting the $D^{*+}K^\pm\mu^-\bar{\nu}_\mu$ control sample. A similar simulated sample is also used to generate kinematic distributions for final states containing a tertiary muon from $\bar{B}^0 \to D^{*+}D_sX$ where D_s decays semileptonically.

Other background contributions arise from hadrons misidentified as muons and from random combination of a μ^- and a true D^{*+}, or viceversa. Templates for all these contributions are also modeled from data using several control samples, in particular the combinations of D^* and muons with same charge.

In Figure 2 the fit results are presented: in particular the figure shows the distribution of m^2_{miss} and E^* separated in four bins of q^2 together with the fit function.

The fit determines the yields fraction of signal with respect to normalization channel $N(\bar{B}^0 \to D^{*+}\tau^-\bar{\nu}_\tau)/N(\bar{B}^0 \to D^{*+}\mu^-\bar{\nu}_\mu) = (4.54 \pm 0.46)\%$, where the error is due to data an Monte Carlo statistics and to the variation of the form factors . Accounting for $\varepsilon_\tau/\varepsilon_\mu$ and the branching ratio $\mathscr{B}(\tau^- \to \mu^-\bar{\nu}_\mu\nu_\tau)$ the $R(D^*)$ value can be obtained.

Several sources of possible systematic uncertainties related to modeling of the templates and to the normalization are considered. They are summarized in Figure 3 and the total systematic uncertainty amounts to 3%.

The largest systematics contributions are due to the limited size of the simulated sample and due to the uncertainty in the shape of the template describing the component of hadrons misidentified as muons. The latter is determined by comparing the result of two different method to

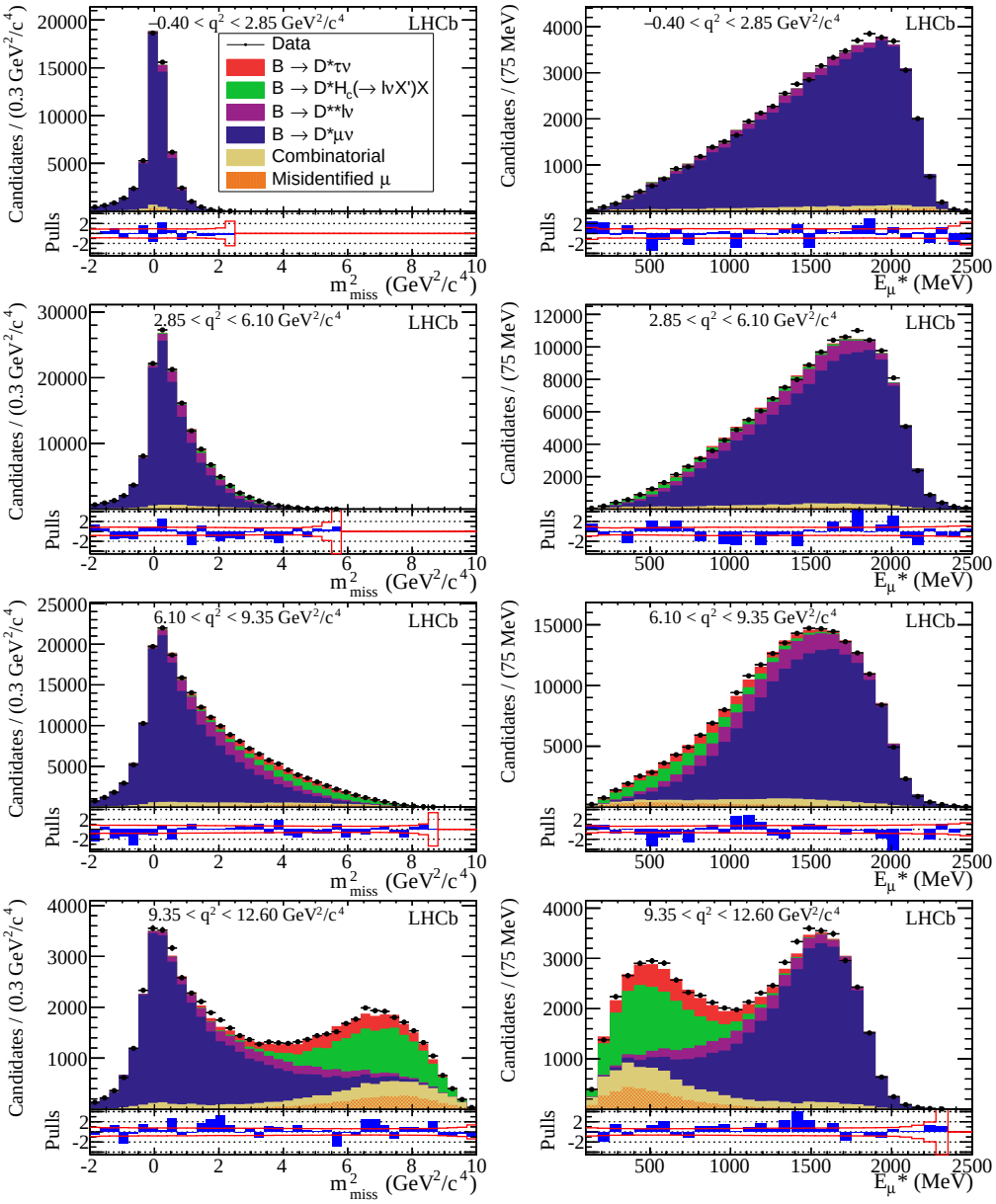

Figure 2: Distributions of m^2_{miss} (left) and E^* (right) of the four q^2 bins of the signal data, overlaid with projections of the fit model with all normalization and shape parameters at their best-fit values. Below each panel differences between the data and fit are shown, normalized by the Poisson uncertainty in the data. The bands give the 1σ template uncertainties [14].

extract the shape. Uncertainties related to the normalization are small because they affect both $\bar{B}^0 \to D^{*+}\tau^-\bar{\nu}_\tau$ and $\bar{B}^0 \to D^{*+}\mu^-\bar{\nu}_\mu$ branching fractions in similar way and then cancel out in the ratio. Many other contributions are due to size of data control sample, hence they will decrease in the future with more data collected by LHCb.

In conclusion, LHCb has measured the ratio of branching fractions:

Model uncertainties	**Absolute size ($\times 10^{-2}$)**
Simulated sample size	2.0
Misidentified μ template shape	1.6
$\overline{B}^0 \to D^{*+}(\tau^-/\mu^-)\overline{\nu}$ form factors	0.6
$\overline{B} \to D^{*+}H_c(\to \mu\nu X')X$ shape corrections	0.5
$\mathcal{B}(\overline{B} \to D^{**}\tau^-\overline{\nu}_\tau)/\mathcal{B}(\overline{B} \to D^{**}\mu^-\overline{\nu}_\mu)$	0.5
$\overline{B} \to D^{**}(\to D^*\pi\pi)\mu\nu$ shape corrections	0.4
Corrections to simulation	0.4
Combinatorial background shape	0.3
$\overline{B} \to D^{**}(\to D^{*+}\pi)\mu^-\overline{\nu}_\mu$ form factors	0.3
$\overline{B} \to D^{*+}(D_s \to \tau\nu)X$ fraction	0.1
Total model uncertainty	**2.8**
Normalization uncertainties	**Absolute size ($\times 10^{-2}$)**
Simulated sample size	0.6
Hardware trigger efficiency	0.6
Particle identification efficiencies	0.3
Form-factors	0.2
$\mathcal{B}(\tau^- \to \mu^-\overline{\nu}_\mu\nu_\tau)$	< 0.1
Total normalization uncertainty	**0.9**
Total systematic uncertainty	**3.0**

Figure 3: Systematic uncertainties in the extraction of $R(D^*)$ [14].

$$R(D^*) \equiv \frac{\mathscr{B}(\bar{B}^0 \to D^{*+}\tau^-\bar{\nu}_\tau)}{\mathscr{B}(\bar{B}^0 \to D^{*+}\mu^-\bar{\nu}_\mu)} = 0.336 \pm 0.027\ (stat) \pm 0.030\ (syst).$$

In Fig. 4 the prospect of all $R(D^*)$ and of $R(D)$ measurements is shown. The LHCb measurement results are in good agreement with the others and it is 2.1 standard deviations greater than the Standard Model expectation. The HFAG (winter 2016) average of $R(D^*)$ and of $R(D)$ measurements, including correlations, is 4 standard deviations from Standard Model prediction.

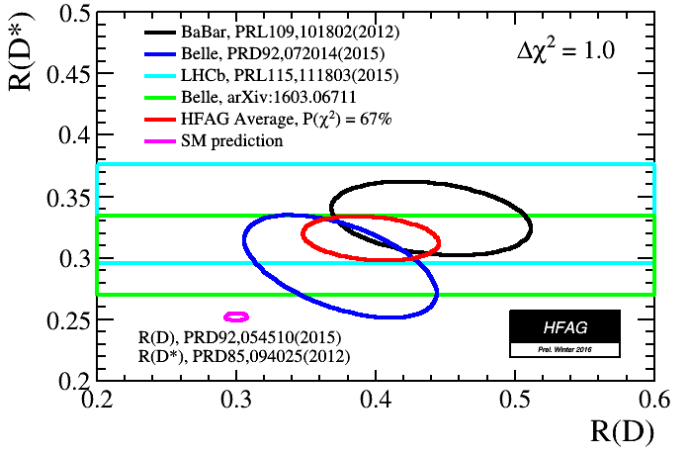

Figure 4: Average of $R(D^*)$ and of $R(D)$ measurements, HFAG group, winter 2016

References

[1] LHCb Collaboration, Aaij, Roel et al., *Test of lepton universality using $B^+ \to K^+\ell^+\ell^-$ decays,* *Phys. Rev. Lett.* **113** (2014) 151601 [arXiv:1406.6482]

[2] M. Tanaka, *Charged Higgs effects on exclusive semitauonic B decays,* *Z. Phys.* C **67** 321 (1995)

[3] S. Fajfer, J. F. Kamenik and I. Nisandzic, *On the $B \to D^* \tau \bar{\nu}_\tau$ Sensitivity to New Physics,* *Phys. Rev. D* **85**, 094025 (2012) [arXiv:1203.2654]

[4] K. A. Olive *et al., [Particle Data Group Collaboration], Review of Particle Physics,* *Chin. Phys. C* **38** (2014) 090001.

[5] BaBar Collaboration, J. P. Lees et al., *Measurement of an Excess of $\bar{B} \to D^{(*)} \tau^- \bar{\nu}_\tau$ Decays and Implications for Charged Higgs Bosons,* *Phys. Rev. D* **88**, no. 7, 072012 (2013)

[6] Belle Collaboration, A. Bozek et al., *Observation of $B^+ \to \bar{D}^{*0} \tau^+ \nu_\tau$ and Evidence for $B^+ \to \bar{D}^0 \tau^+ \nu_\tau$ at Belle,* *Phys. Rev. D* **82** (2010) 072005

[7] LHCb Collaboration, Alves et al., *The LHCb Detector at the LHC,* *JINST* **3** (2008) S08005

[8] LHCb Collaboration, Aaij, Roel et al., *LHCb Detector Performance,* *Int. J. Mod. Phys. A30* **07** (2015) 1530022

[9] LHCb Collaboration, Aaij, Roel et al., *Performance of the LHCb Vertex Locator,* *JINST* **9** (2014) 09007

[10] LHCb Outer Tracker Group Collaboration, Arink, R et al, *Performance of the LHCb Outer Tracker,* *JINST* **01** (2014) 9

[11] LHCb RICH Group Collaboration, Adinolfi, M. et al, *Performance of the LHCb RICH detector at the LHC,* *Eur. Phys. J.* **C73** (2013) 2431

[12] LHCb Collaboration, Alves et al., *Performance of the LHCb muon system,* *JINST* **8** (2013)

[13] LHCb Collaboration, Alves et al., *The LHCb Trigger and its Performance in 2011,* *JINST* **8** (2013)

[14] LHCb Collaboration, Aaij et al., *Measurement of the Ratio of Branching Fractions $\mathscr{B}(\bar{B}^0 \to D^{*+}\tau^-\bar{\nu}_\tau)/\mathscr{B}(\bar{B}^0 \to D^{*+}\mu^-\bar{\nu}_\mu)$,* *Phys. Rev. Lett.* **115** (2015) 111803

[15] I. Caprini, L. Lellouch and M. Neubert., *Dispersive bounds on the shape of anti-B $\to$ D(*) lepton anti-neutrino form-factors,* *Nucl. Phys. B* **530** (1998) 153

[16] R.Barlow and C.Beeston, *Fitting using finite Monte Carlo sample,* *Computer Physics Communications* **77** (1993)

[17] A. K. Leibovich, Z. Ligeti, I. W. Stewart and M. B. Wise, *Semileptonic B decays to excited charmed mesons,* *Phys. Rev. D* **57** (1998) 308

[18] N. Isgur and M. B. Wise, *Weak decays of heavy mesons in the static quark approximation,* *Phys. Lett. B* **232** (1989) B113